Acta Montanistica Slovaca
ISSN 1335-1788
actamont.tuke.sk

Impact of Discrete Fracture Characteristics on Longwall Top Coal Stability

Tien Dung LE[1]*, Hong Quang DAO[2]** and **Dinh Hieu VU[3]

Authors' affiliations and addresses:
[1] Department of Underground Mining, Hanoi University of Mining and Geology, 18 Pho Vien, Duc Thang, Bac Tu Liem, Hanoi 100000, Vietnam
e-mail: t.d.le@humg.edu.vn
https://orcid.org/0000-0002-0212-888X

[2] Institute of Mining Science and Technology, VINACOMIN, 3 Phan Dinh Giot, Phuong Liet, Thanh Xuan, Hanoi 100000, Vietnam
e-mail: daohongquang@gmail.com

[3] Vietnam Institute of Seas and Islands, Vietnam Administration of Seas and Islands, 67 Chien Thang, Van Quan, Ha Dong, Hanoi 100000, Vietnam
e-mail: vudinhhieu@gmail.com

***Correspondence:**
Tien Dung Le, Department of Underground Mining, Hanoi University of Mining and Geology, 18 Pho Vien, Duc Thang, Bac Tu Liem, Hanoi 100000, Vietnam
tel.: +84 98 695 7677
e-mail: t.d.le@humg.edu.vn
https://orcid.org/0000-0002-0212-888X

Funding information:
Funding Agency: Vietnam National Foundation for Science and Technology Development (NAFOSTED)
Grant Number: 105.08-2019.09

Acknowledgement:
This research is funded by Vietnam National Foundation for Science and Technology Development (NAFOSTED) under grant number 105.08-2019.09.

How to cite this article:
Le, T.D. Dao, H.Q. and Vu, D.H. (2022). Impact of Discrete Fracture Characteristics on Longwall Top Coal Stability. *Acta Montanistica Slovaca*, Volume 27 (4), 851-863.

DOI:
https://doi.org/10.46544/AMS.v27i4.02

Abstract
Discrete fractures may exist in thick coal seam and significantly impact the top coal stability in the Longwall Top Coal Caving method (LTCC) both ahead of shield support (top coal fall) and behind shield support (top coal caving). The top coal stability in such conditions is not well understood in the literature and has been studied from either fall or caving behaviour. In this paper, a discontinuum-based numerical program is used to study longwall top coal stability when discrete fractures exist in coal seam and vary in characteristics (i.e., orientation, density, stiffness, strength, and intersecting fractures). The study demonstrates that the existence of discrete fractures decreases the top coal stability ahead of shield support, particularly in initial face extraction. The parametric study finds that when the fracture orientation makes an angle of 90 degrees to the positive x-axis, it has the least impact on top coal fall. When the fractures plunge into the mined-out area, they facilitate top coal caving and vice versa when they plunge into the unmined area. The study reveals that the fracture density is directly proportional to top coal fall and top coal caving. Meanwhile, the fracture stiffness and strength are inversely proportional to both top coal fall and caving. The study also demonstrates the important role of coal seam characteristics (strength, elastic modulus, and depth) in top coal fall. The findings from this paper can assist engineers in improving panel geometry design and roof control for efficient underground mining when discrete fractures exist and vary in a coal seam.

Keywords
Top coal fall; Top coal caving; Fracture orientation; Fracture density; Intersecting fractures.

Introduction

Longwall Top Coal Caving (LTCC), due to its significant improvement of equipment in recent decades, has been widely used to efficiently extract thick coal seam from Europe to America, Asia, Oceania, and Africa. Two fundamental geotechnical requirements for the successful operation of LTCC are the maintenance of top coal stability between the coal wall and shield support (top coal ahead of shield support) and the maximisation of top coal caving behind the support (Fig. 1). After each web cut by the shearer, the top coal (or roof) ahead of shield support, if inappropriately supported, may fall onto the shearer, armoured face conveyor and workers at face. If top coal/roof falls excessively or in large lumps, it may break or prevent face equipment from proper working. This results in production interruption from days to weeks and consequently causes significant economic loss. At its worst, top coal fall (or roof fall) may cause injuries to workers and even human loss, as reported in various coal industries such as Belgium (Vervoort, 1988), Poland (Prusek et al., 2017), USA (Iannacchione et al., 2007; Pappas & Mark, 2012), India (Palei & Das, 2008), China (Xu et al., 2015), Vietnam (Le et al., 2020), Australia and South Africa (Payne, 2008; Grey & Gibbons, 2020). A sufficient understanding of top coal behaviours both ahead of and behind shield support is, therefore, of great importance for successful LTCC operation from the perspectives of safety and productivity.

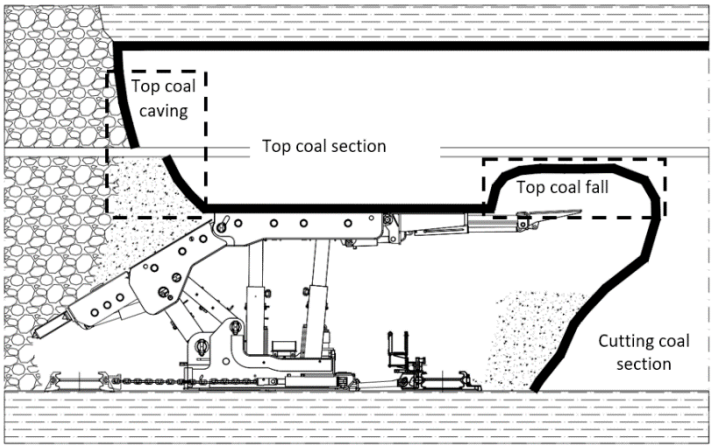

Fig. 1. Conceptual model of top coal fall and top coal caving in LTCC

Since the top coal section in LTCC can theoretically be considered equivalent to the immediate roof in conventional longwall (SPL), top coal fall mechanics can partly be understood from previous SPL roof fall studies. From German mining practice, Langosch et al. (2003) developed an analytical equation for the prediction of roof fall frequency ahead of shield support. The critical distance between the canopy tip and coal wall (tip-to-face distance), thickness and strength of the first roof layer, support resistance, and vertical stress were identified as key parameters controlling the fall. From Australian mining practice, Frith (2005) identified two fundamental mechanics of roof fall (i.e., horizontal stress-driven guttering and delineation of a large block) and three direct relevant factors (i.e., face spall, roof convergence above support, and longwall retreat rate). Using the concept of Euler Buckling, he found that the potential for guttering-type roof fall was a function of panel width and extraction height, while the potential for large block delineation-type roof fall was dependent on the thickness of near-seam massive strata. Also recognising the role of roof convergence in roof fall, Hoyer (2011), Medhurst et al. (2014), and Trueman & Hutchinson (2018) used field monitoring data of leg pressure of shield support to develop tools for early warning of roof fall in large block delineation cases. These tools considered real-time roof stability in which time-dependent strata relaxation and face advance rate were involved. Based on risk assessment methods, Iannacchione et al. (2007) focused on local geological, mining and stress factors to determine roof fall risk in underground mines. Similarly, Prusek et al. (2017) considered roof strata condition plus support characteristics, panel geometry and fault orientation as controlling parameters of roof fall. Alternatively, Rajwa et al. (2020) used the numerical modelling method to study the effect of the geometrical configuration of shield support (i.e., shield capacity distribution, tip-to-face distance) on roof fall possibility. The effect of support structure and capacity was also studied by using an analytical or physical method, as seen in Yang et al. (2017a) and Jasiulek et al. (2019). In general, the above fundamental mechanics and controlling parameters of roof fall in SPL can be used to explain the top coal fall in LTCC to some extent. However, care must be taken for the use because top coal contains more bedding planes and is commonly weaker, whereas immediate roof contains fewer bedding planes and is commonly stronger.

To the best of the authors' knowledge, the top coal fall ahead of shield support was investigated in a few LTCC studies (Le et al., 2018; Hebblewhite et al., 2002; Le et al., 2020). These studies and SPL studies mostly focused on coal-measure rocks containing bedding planes and parallel joint sets. Apart from these typical

structures, a coal seam may contain discrete fractures which constitute a unique network (Cao, 2019). These fractures may significantly impact top coal stability because their characteristics commonly vary in practice. This impact is, however, not well understood in the literature. Besides, many top coal/roof fall studies did not consider the top coal/roof caving behind shield support. This reduces the reliability and accuracy in the assessment of LTCC/SPL efficiency in those studies. The reader is referred to Le et al. (2017) and Wang et al. (2020) for more detailed studies on longwall top coal caving.

This paper presents a detailed study of longwall top coal stability when discrete fractures exist in coal seam and vary in characteristics (i.e., orientation, density, stiffness, strength, and intersecting fractures). The stability in different coal seam characteristics (i.e., strength, elastic modulus, and depth) is also investigated. The discrete fractures, along with typical vertical joints and horizontal bedding planes, are modelled in an LTCC model by using a discontinuum-based numerical program. The top coal fall is analysed jointly with the top coal caving. A better understanding of top coal stability from this paper can assist engineers in improving panel geometry design and top coal control for efficient LTCC operation when discrete fractures exist and vary in the coal seam.

Discontinuum Modelling of Longwall with Discrete Fractures

Because top coal fall and top coal caving in LTCC involve the failure, displacement, rotation and complete detachment of highly jointed rock materials, a discontinuum-based numerical program (UDEC developed by Itasca Consulting Group (2019)) was selected for the study for two main reasons. First, compared to empirical and analytical methods, a numerical method can provide a detailed investigation into the micro- and macro-behaviours of different rock masses associated with progressive longwall mining under various geological conditions within reasonable time periods. Second, a discontinuum-based method, compared to the continuum-based method, is more efficient and stable in incorporating many geological structures (discontinuities), recognising new contacts, and rotating and detaching discrete blocks (Itasca Consulting Group, 2019). Although UDEC is a two-dimensional program in nature, it - with plane-strain modelling condition - can capture the mechanics of longwall geotechnical problems along panel strike because the mining along panel strike direction is normally much greater than that along panel dip direction.

Geological condition and model geometry

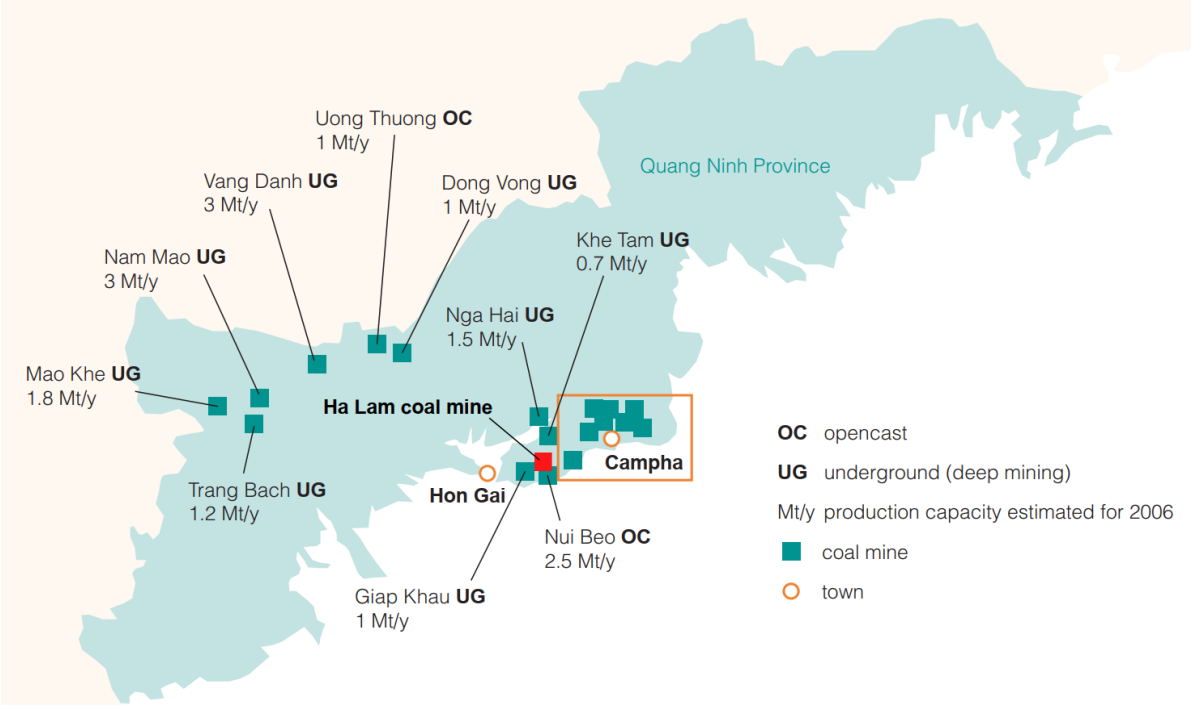

Fig. 2a. Location of Ha Lam coal mine (modified from Paul, 2010)

The geological condition of Seam 11, Ha Lam coal mine, Quang Ninh coalfield, Vietnam (Fig. 2a), was used for developing an LTCC model because an on-site LTCC face has been operated in this relatively weak and fractured coal seam. Based on a cross-section along Seam 11's strike direction (Fig. 2b), the seam was modelled at a depth of 200 m below the surface. The seam was considered flat because it had an average dip angle of less than 10 degrees at the field. Based on the geological document of the company (Ha Lam Coal Company, 2015), the coal seam, immediate roof strata and main roof strata thicknesses were 8.0, 8.5 and 16.5 m in the model,

respectively. The floor and overburden strata were modelled with the same thickness of 50 m. The rest of the overburden strata (125 m) was implicitly represented through vertical stress of 3.25 MPa applied on the top boundary of the model. The total model dimension along the panel strike (150 m) was 3.0 times the extraction dimension (50 m). Typical structures within top coal seam, such as bedding planes and vertical joints, were modelled with an average spacing of 0.5 m based on caved coal lump size at the field and due to computation time limit. The bedding plane and joint spacings were increased from the area of interest (extraction area) to the outer area. The geological document of the company (Ha Lam Coal Company, 2015) shows that Seam 11 contains a discrete fracture network whose orientation distribution is nearly the same as that of a mine-scale fault network. Therefore, the discrete fractures were modelled by using Gaussian distribution with a mean dip angle of 115 degrees (from the positive x-axis) and a standard deviation of 10. The fractures extended through the whole coal seam thickness with a density of 0.5 m/m^2, as observed and estimated at the field. Due to limited underground observation space, the fracture network's position and size were modelled using uniform distributions for simplification. The geometry of the LTCC model is shown in Fig. 3.

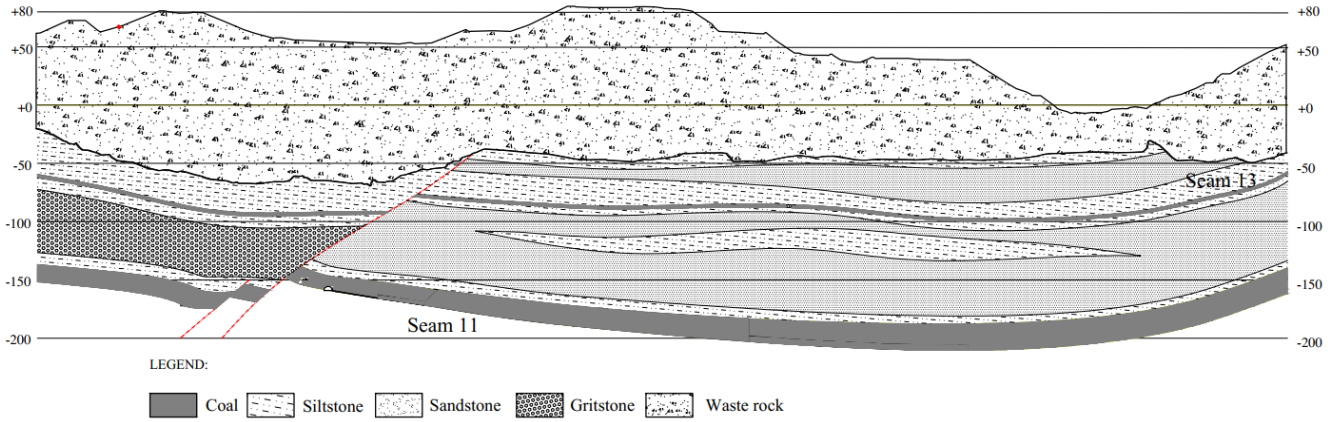

Fig. 2b. Geological cross-section along Seam 11's strike direction, Ha Lam coal mine (north-northwest to south-southeast) (modified from Ha Lam Coal Company, 2015)

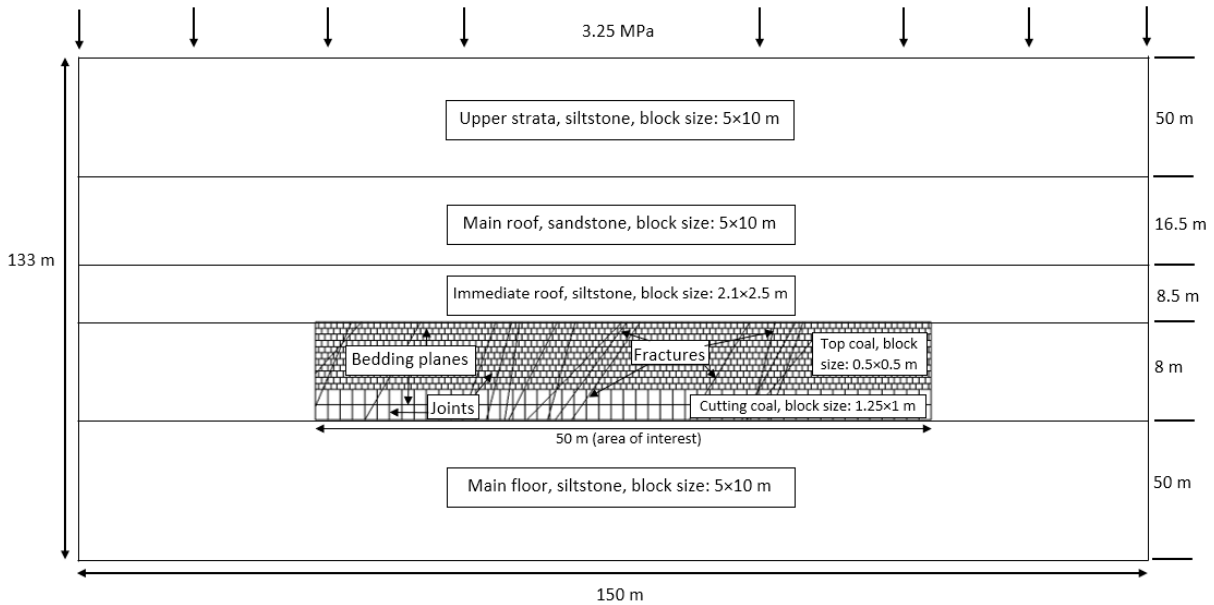

Fig. 3. The geometry of the LTCC model with geological structures in the area of interest

Block and discontinuity properties

The strain-softening and Coulomb slip laws were assigned to intact blocks and discontinuities (bedding planes, joints, fractures), respectively. The strain-softening law was capable of modelling material failure and strength reduction during top coal fall/caving. An attempt was made to collect and test coal samples from the Ha Lam coal mine. However, the laboratory test results were significantly impacted by small cracks in the samples despite careful preparation. Hence, the properties of rock materials of the mine were adopted from Le et al. (2018), in which the properties were derived from available test results for the Quang Ninh coalfield (Pham, 2012; Ha Lam Coal Company, 2015), empirical scaling factors for sedimentary rocks (McNally, 1996; Mohammad et al.,

1997; Vakili et al., 2012) and UDEC developer's recommendations for unknown parameters (Itasca Consulting Group, 2019). For example, the rock material strength was derived from corresponding laboratory strength by using a reduction factor of 5. The deformation modulus and tensile strength were derived from their laboratory values by using a reduction factor of 2.13 and 2.0, respectively. The residual cohesion and tensile strengths were 20 and 10%, respectively, of their peak strengths. The discontinuity shear strength increased from coal to siltstone to sandstone, while its tensile strength was assumed to be zero in all strata. Note that bedding planes, joints and fractures were assumed to have the same properties within each rock material. The block and discontinuity properties assigned to the LTCC model are presented in Table 1.

Tab. 1. Block and discontinuity properties assigned to LTCC model (adopted from Le et al., 2018)

Material	Block properties							
	Cohesion [MPa]	Friction [degree]	Bulk modulus [GPa]	Shear modulus [GPa]	Tensile strength [MPa]	Residual cohesion [MPa]	Residual tensile strength [MPa]	Critical strain [%]
Coal	1.52	32	1.21	0.73	1.55	0.304	0.155	0.5
Siltstone	4.73	32	3.83	2.29	3.05	0.945	0.305	0.1
sandstone	9.15	34	7.43	4.46	5.25	1.83	0.525	0.1
Material	Discontinuity properties							
	Normal stiffness [GPa/m]	Shear stiffness [GPa/m]	Cohesion [MPa]	Friction [degree]	Tensile strength [MPa]	-	-	-
Coal	10	1	0	15	0	-	-	-
Siltstone	10	1	0	20	0	-	-	-
sandstone	10	1	0	25	0	-	-	-

Model calibration and verification

Each mining cycle was modelled by removing a 1 m thick coal wall, advancing shield support to the new coal wall, and running the model to reach an equilibrium state. To minimise any errors in numerical result caused by the uncertainties in model development, the model was calibrated against the top coal stability in initial extraction observed at the field. This stability was manifested as the face distance out of the installation room where the top coal started to cave (face distance of top coal first caving). According to on-site engineers, this face distance was observed at the field to be 6–8 m when the area contained no discrete fractures. When the area contained fractures, as in the case being studied, top coal was observed to start caving as soon as the face advanced out of the installation room. The calibration was performed by adjusting the damping parameters in UDEC in a trial-and-error process. After calibration, the model well represented the top coal stability behaviour in the two cases (with and without discrete fractures), as described in the next section. When the model reached a cyclic extraction, the failure extent of the coal seam was about 20 m ahead of the coal wall (Fig. 4). This value fell within the failure extent observed by the engineers (20–25 m), verifying the validity of the model. The LTCC model was named the "benchmark model" for parametric study in the next sections.

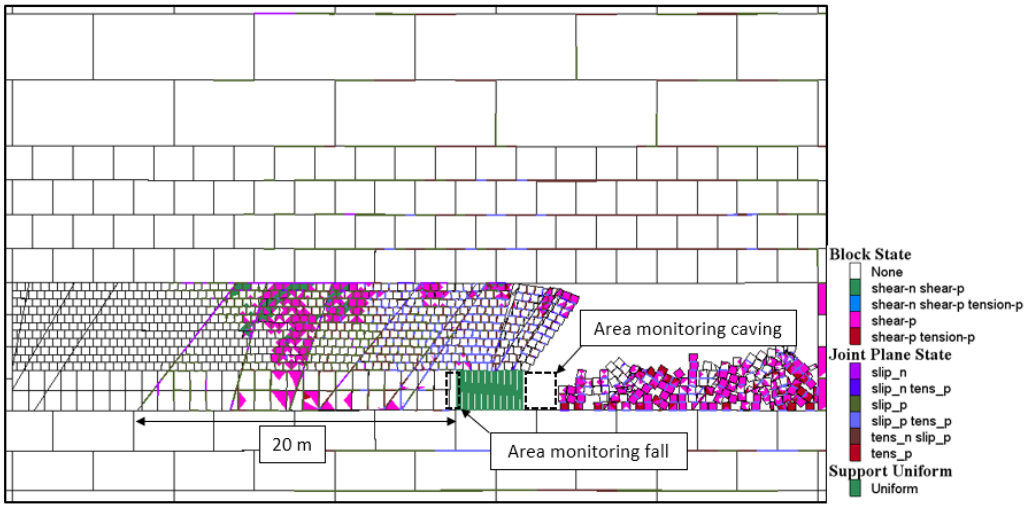

Fig. 4. Failure extent of coal seam and monitoring areas of stability

Impact of Fracture Characteristics on Top Coal Stability

Based on the benchmark model, the top coal fall and caving behaviours under possible variations of fracture characteristics were studied. This was implemented by changing the input value of the analysed characteristic while keeping the other characteristics' value unchanged. The fracture characteristics such as orientation, density,

stiffness, and friction were studied because they can facilitate or impede the fall/caving by changing the potential path of coal/rock displacement, shape and size of coal/rock block, and overall strength/stiffness of coal seam. Besides, because the underground observation was limited, as mentioned earlier, only one set of discrete fractures was observed and modelled in the benchmark model. In cases in which two or more fracture networks exist and intersect with each other (intersecting fractures), the response of the coal seam becomes complicated (Peng, 2008). The impact of the existence and orientation of intersecting fractures on top coal stability was therefore studied in this section.

Several indices of top coal stability were developed as follows. First, the top coal fall was manifested through a top coal fall rate (%). The rate was calculated by dividing the total number of top coal blocks that fell into the area monitoring fall during extraction by the total number of pre-mining top coal blocks in 10 m of extraction. Second, the top coal caving was manifested through a top coal recovery rate (%). The rate was calculated by dividing the total number of top coal blocks caved into the area monitoring caving by the total number of pre-mining top coal blocks. This calculation was for 30 m of extraction at the model centre. Third, top coal discontinuity failure was manifested through discontinuity failure rates in tension and shear. For example, the discontinuity failure rate in tension was calculated by dividing the total number of top coal discontinuities ahead of the coal wall failed in tension at 22 m of face advance by the total number of top coal discontinuities in 22 m of extraction. The areas monitoring fall and caving are illustrated in Fig. 4. The monitoring was automatically implemented in every mining cycle by using user-defined FISH (a built-in programming language in UDEC) functions.

Fracture existence

To understand the impact of the existence of discrete fractures on top coal stability, another LTCC model having similar settings to the benchmark model but without discrete fractures was developed. The numerical results show that in initial extraction, the top coal in the no-fracture model started to cave at 9 m of face advance, while it in the benchmark model caved as soon as the face advanced out of the installation room (Fig. 5). These results are consistent with the field observations presented in the previous section. After 50 m of extraction, the top coal between the coal wall and shield support did not fall in the no-fracture model (the top coal fall rate was zero), while it fell with a rate of 16.69% in the benchmark model. The discontinuity failure rates in tension and shear in the no-fracture model (6.04 and 19.83%, respectively) were less than those in the benchmark model (15.08 and 42.90%, respectively). The numerical results demonstrate that the existence of fractures made the coal seam weaker, reducing the top coal stability ahead of shield support. The fractures also split top coal blocks into smaller blocks that were easier to fall.

Behind shield support, the top coal recovery rate in the no-fracture model (59.98%) was slightly less than that in the benchmark model (60.35%). Although the coal seam became weaker when fractures existed, the top coal behind support had already failed, and its caving was slightly impacted by the seam strength reduction. As analysed in the next subsection, the fracture orientation also impacted top coal caving.

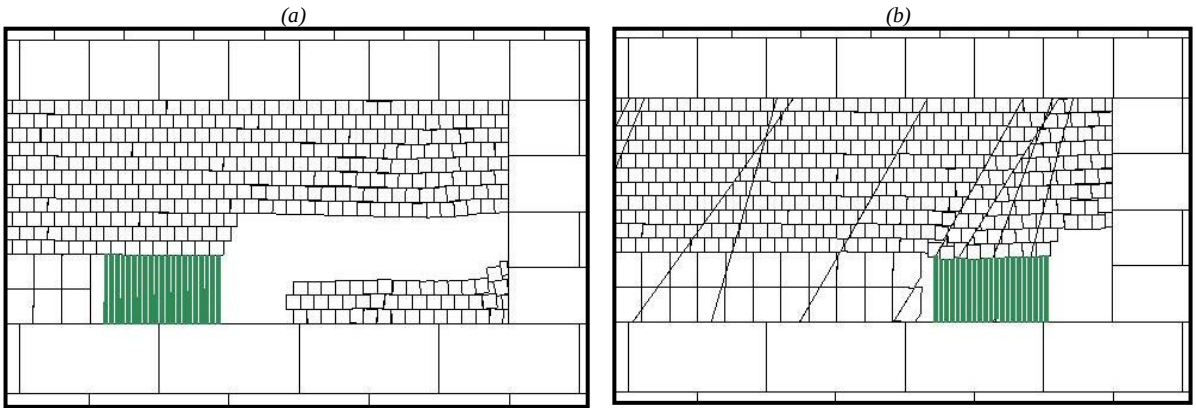

Fig. 5. Top coal stability at (a) 9 m of face advance in the no-fracture model and (b) 1 m of face advance in the benchmark model

Fracture orientation

Five different fracture orientations were modelled to cover the possible range of 45–135 degrees of the field orientation. The top coal fall, discontinuity failure in tension, discontinuity failure in shear, and top coal recovery rates are shown in Fig. 6. The figure shows that ahead of shield support, the top coal fall, discontinuity failure in tension, and discontinuity failure in shear rates in the 90-degree fracture orientation model (7.23, 4.36 and 18.91%, respectively) were all smaller than the corresponding rates in the other models. This means that the top coal was the most stable in the 90-degree fracture orientation model. The result also indicates that the coal seam was strongest when the fractures reached an angle of 0 degrees with vertical loading from overburdened strata.

The impact of this fracture orientation agrees with the impact of joint orientation on coal strength documented in Peng (2008) and Yang et al. (2017b). The top coal was less stable for the non-vertical fracture orientation models when the fractures plunged into the mined-out area. In particular, the top coal fall rate was greatest in the 65-degree fracture orientation model (38.27%). Meanwhile, the discontinuity failure rates in tension and shear were greatest in the 45-degree fracture orientation model (29.14 and 63.64%, respectively).

Behind shield support, the top coal recovery rates in the 45- and 65-degree fracture orientation models (92.16 and 91.58%, respectively) were significantly greater than those in the 115- and 135-degree fracture orientation models (60.35 and 64.91%, respectively). There are two possible causes. First, the top coal portion above fractures had more free space to displace downwards in the first two models as the fractures plunged into the mined-out area, while it had less free space for displacement in the last two models as the fractures plunged into the unmined area. Second, when a fracture plunges into the unmined area, it may act as a caving line along which some top coal bocks could fall behind the recovery area. This contributes to the lower recovery rate, as mentioned above.

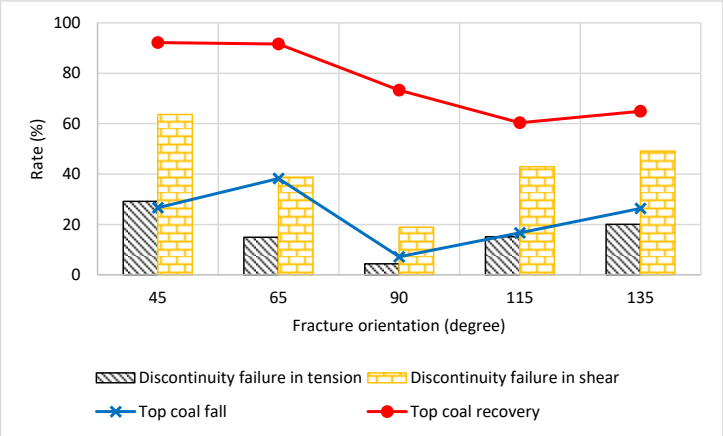

Fig. 6. Top coal stability in different fracture orientations

Fracture density

Four different fracture densities were modelled to represent an increase in the total length of fractures from 0.5 to 2 m per square meter in the area of interest. It can be seen from Fig. 7 that as the fracture density increased, the top coal fall and discontinuity failure rates followed an increasing trend. The top coal fall rate increased from 16.69 to 37.62%, while discontinuity failure rates in tension and shear increased from 15.08 and 42.90 to 39.87 and 78.63%, respectively. This means that the top coal ahead of shield support became less stable. The reason was that when the density increased, more number and length of fractures were added into the models that, according to the fracture mechanics theory, made the coal seam weaker. Behind shield support, the top coal recovery rate increased from 60.35 to 68.55%. As discussed above, the increase can also be attributed to the weaker seam. However, the caving line was theoretically unchanged because the fracture orientation remained unchanged. The top coal recovery rate was therefore increased moderately.

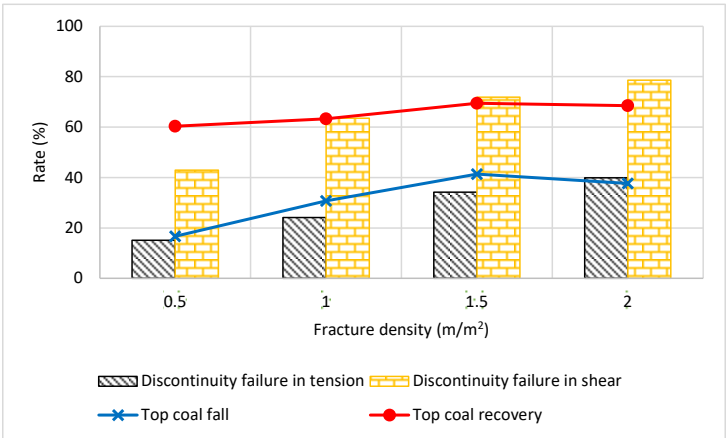

Fig. 7. Top coal stability in different fracture densities

Fracture stiffness and strength

Four different stiffnesses of fracture (both normal and shear with a constant normal-to-shear stiffness ratio) were modelled to represent a wide range of fracture stiffness as the stiffness was not available from the practice.

Figure 8 shows that when the normal stiffness increased from 1 to 20 GPa/m (shear stiffness increased from 0.1 to 2 GPa/m accordingly), the top coal fall and top coal recovery rates decreased from 25.40 and 68.34% to 15.24 and 59.02%, respectively. These numerical results indicate an increase in top coal stability both ahead of and behind shield support. The results can be explained by fracture displacement as follows. When subjected to the same stress regime, a fracture with higher stiffness has better displacement resistance than a fracture with lower stiffness. Hence, the models' top coal blocks adjacent to a stiffer fracture were limited in displacement, which caused less block fall and caving. It should be noted that the stiffness did not much impact the discontinuity failure rates (in both tension and shear) because the fracture strength was kept constant in the models.

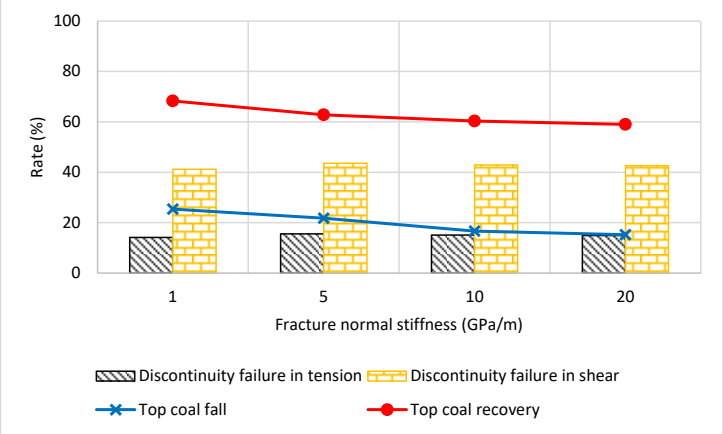

Fig. 8. Top coal stability in different fracture stiffnesses

Four different fracture friction angles were modelled to cover the possible range of 5–35 degrees of friction at the field. Figure 9 shows that when the fracture friction increased, the top coal fall rate, discontinuity failure in tension rate and discontinuity failure in shear rate clearly decreased from 30.48, 18.27 and 51.70% to 4.35, 6.95 and 25.13%, respectively. The decrease can be straightforwardly explained that when the fracture friction angle increased, its strength and, consequently, coal seam strength also increased, which impeded fracture failure and block fall. These results confirm that stronger fracture clearly increases the top coal stability ahead of shield support. Behind shield support, the top coal recovery rate also decreased from 71 to 57.93%. This impact of fracture strength on top coal caving agrees with the impact of joint strength on the caving in Rafiee et al. (2018). It should be noted that the impact of fracture strength on discontinuity failure was clearly observed, as opposed to the impact of fracture stiffness on the failure.

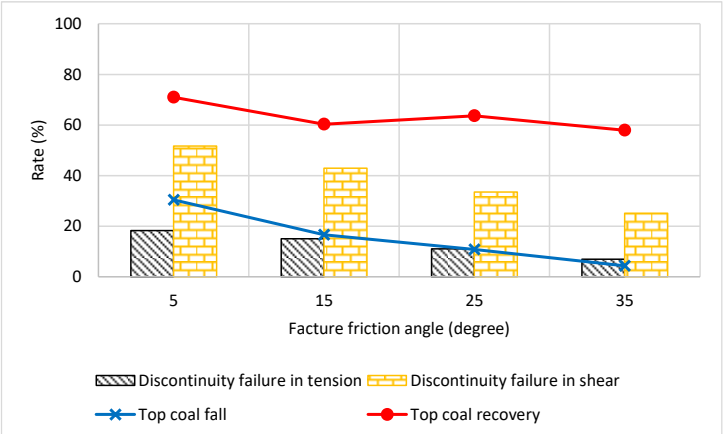

Fig. 9. Top coal stability in different fracture friction angles

Intersecting fractures

This paper presents four simple cases based on the benchmark model in which a second discrete fracture network exists and varies in its orientation from 65 to 130 degrees with a constant standard deviation of 10 (Fig. 10a–d). The top coal stability during LTCC extraction in the four models and benchmark model is presented in Fig. 11. As expected, the existence of the second fracture network made the coal seam weaker, and the top coal became less stable. The top coal fall, discontinuity failure in tension, discontinuity failure in shear and top coal recovery rates (25.03–32.50, 18.18–29.83, 50.03–65.77 and 61.72–79.56%, respectively) in the two-fracture-network models (intersecting cases) were greater than the corresponding rates (16.69, 15.08, 42.90 and 60.35%,

respectively) in the single-fracture-network model (benchmark model/non-intersecting case). Ahead of shield support in the intersecting cases, the top coal can be considered most stable when the second fracture network's orientation is 90 degrees (Fig. 10b). In this model, although the top coal fall rate (27.93%) was about 2.9% greater than the smallest fall rate (25.03%) in the model in Fig. 10a, the discontinuity failure rates in tension and shear (18.18 and 50.03%, respectively) were less than those in other models (20.91–29.83 and 53.55–65.77%, respectively). Behind shield support, the top coal recovery rate was greatest in the model in Fig. 10a (79.56%). This is because the second fracture network plunged into the mined-out area (while it plunged into the unmined area in other models). As explained earlier, top coal had more free space to displace downward, resulting in a greater recovery rate. The stability characteristics here are consistent with those obtained in the second subsection of this section.

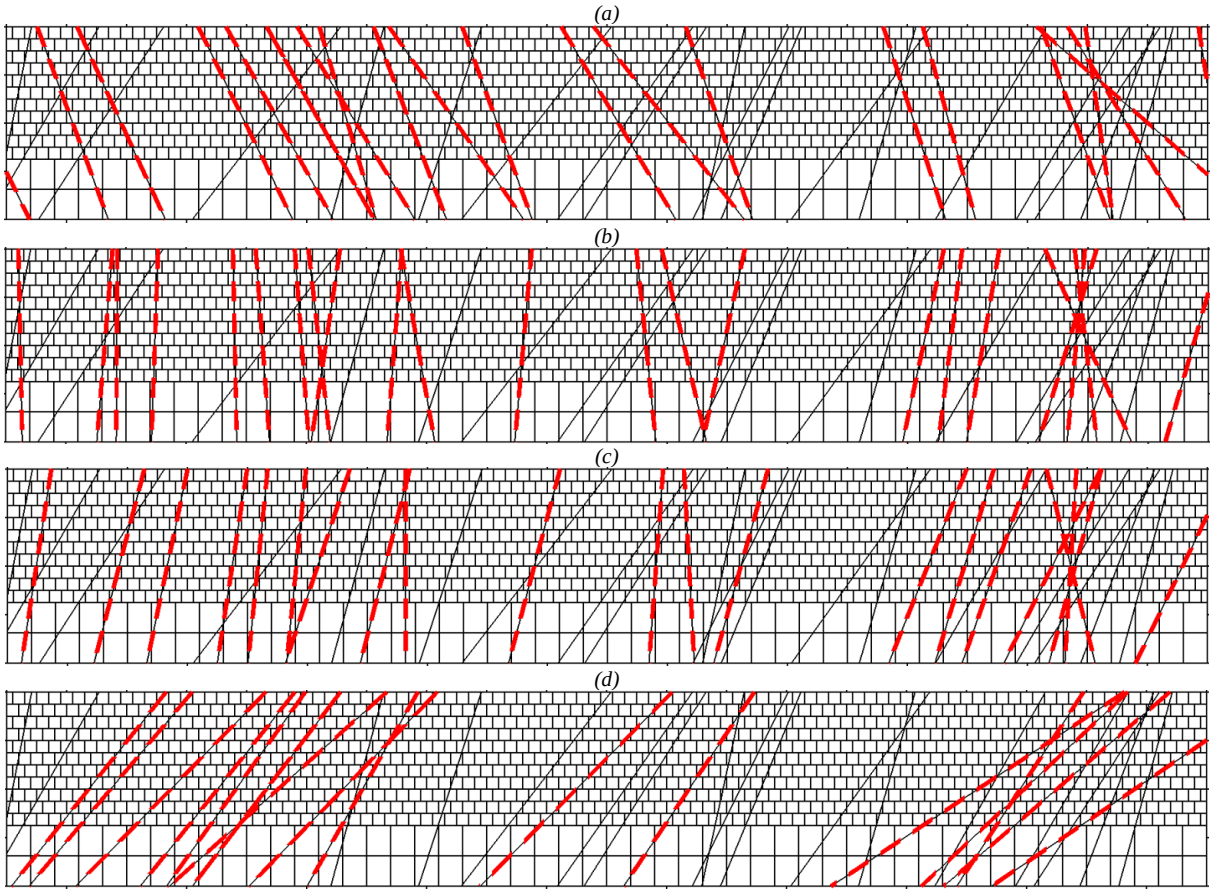

Fig. 10. Coal seam contains second fracture network (dashed line) in (a) 65, (b) 90, (c) 100 and (d) 130 degrees

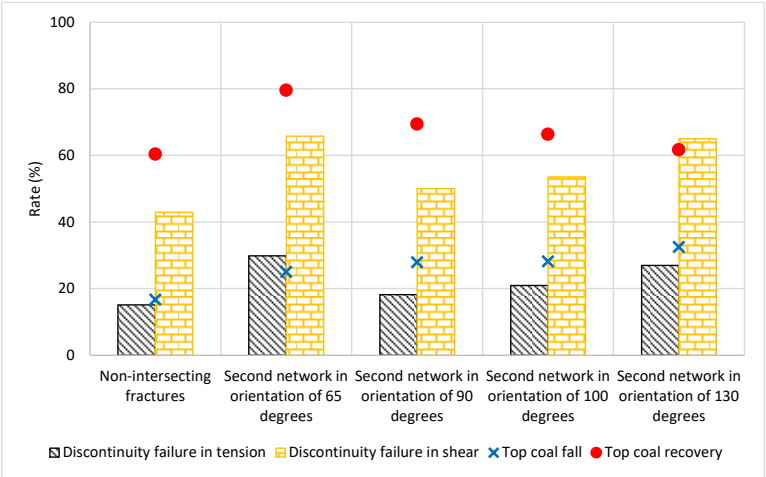

Fig. 11. Top coal stability in non-intersecting and intersecting fractures

Impact of Coal Seam Characteristics on Top Coal Stability

Coal seam strength

Five different coal strengths were modelled to cover the field strength range of 2.74–13.7 MPa. It can be seen from Fig. 12 that ahead of shield support, as the coal strength increased, the top coal fall rate decreased from 25.40 to 10.16%. At the same time, the discontinuity failure rates in tension and shear also decreased from 17.46 and 52.11% to 8.77 and 23.59%, respectively. The decrease can be straightforwardly explained that a stronger coal seam resulted in less seam failure and, accordingly, less block fall. The results confirm that a stronger coal seam increased its stability, particularly in top coal ahead of shield support. However, behind shield support, an increase in coal strength did not clearly impact the top coal recovery rate. This impact needs to be further studied with more detailed strength values and a more rigorous simulation algorithm of top coal recovery for a general conclusion.

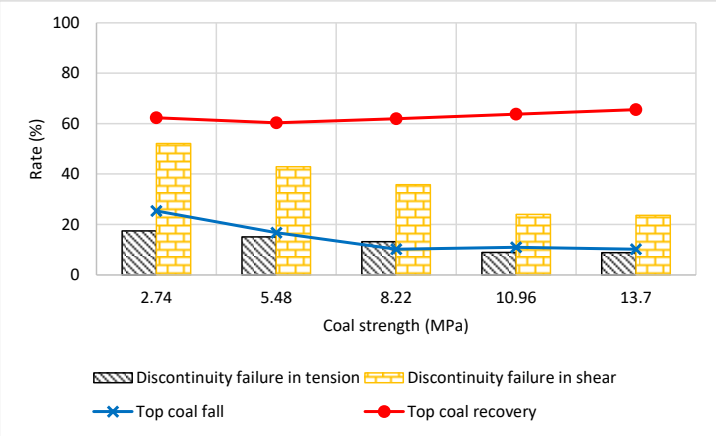

Fig. 12. Top coal stability in different coal strengths

Coal elastic modulus

Five different coal elastic moduli were modelled to cover the field modulus range of 0.61–3.64 GPa. The numerical results are displayed in Fig. 13. As can be seen, ahead of shield support, an increase in coal seam modulus reduced the top coal fall rate (from 36.28 to 14.51%), while it did not show a clear impact on discontinuity failure rates. The reduction in top coal fall rate can be explained by block deformation. When subjected to the same stress regime, a coal block with a higher modulus has better resistance to deformation than a block with a lower modulus. The model's top coal blocks were accordingly more difficult to displace, resulting in less top coal fall. The failure rates of discontinuities were controlled by discontinuity strength and were thus not impacted by coal block elastic modulus. Behind shield support, similar to the top coal fall rate, the top coal recovery rate reduced from 67.37 to 61.56%.

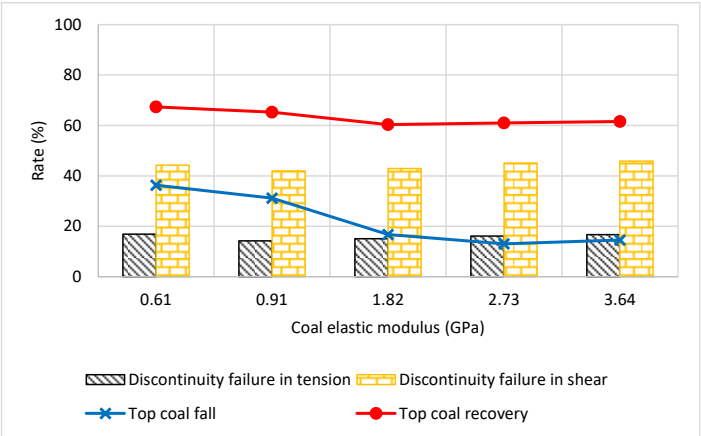

Fig. 13. Top coal stability in different coal seam moduli

Coal seam depth

Four different depths of coal seam were modelled in the range of 100–400 m, and the results are displayed in Fig. 14. The figure clearly shows that ahead of shield support, as the seam depth increased, the top coal fall rate clearly increased from 1.45 to 53.70%. At the same time, the discontinuity failure rates in tension and shear

increased from 9.12 and 24.18 to 15.01 and 50.43%, respectively. The increase can be explained by the fact that as the seam depth increased, the vertical stress increased, facilitating fracture failure and block fall. The results indicate that coal seam depth was directly proportional to top coal fall. However, behind shield support, an increase in coal seam depth did not show a clear impact on the top coal recovery rate. This impact needs to be further studied with more detailed depth values and a more rigorous top coal recovery simulation algorithm for a general conclusion. Note that in a shallow mining condition, the low tensile strength of rock and the presence of many weak geological structures become significant features (Galvin, 2016). Meanwhile, to a certain mining depth, the depth may no longer impact the caving behaviour of top coal (Dao, 2010).

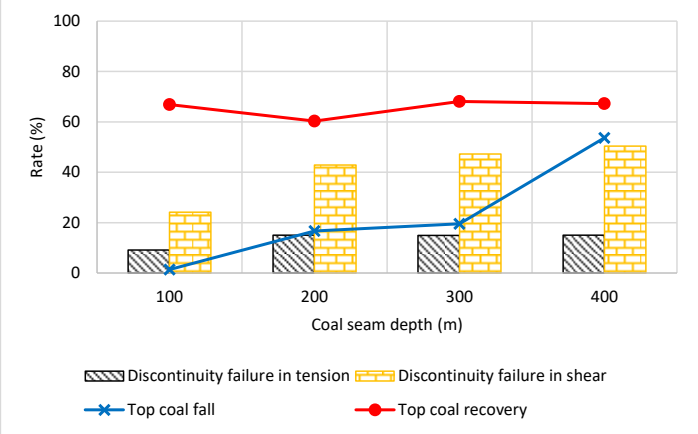

Fig. 14. Top coal stability in different coal seam depths

Discussion and Conclusions

The top coal falling ahead of shield support and top coal caving behind shield support are jointly analysed in this paper. This has not been done in previous longwall top coal/roof stability studies. Accordingly, this paper provides a more comprehensive approach to studying LTCC efficiency because efficiency can be assessed from safety and productivity perspectives. The discontinuum-based numerical program UDEC (Itasca Consulting Group, 2019) allows the realistic representation of discrete fractures and their characteristics' variation, which have not been sufficiently modelled in previous longwall top coal stability studies (Le et al., 2020, Wang et al., 2020, Le et al., 2018, Le et al., 2017, Hebblewhite et al., 2002). In the absence of some geometrical (for instance, fracture position/size distribution) and mechanical (for instance, discontinuity friction/stiffness) properties due to limited space for underground observation or limited laboratory tests, several assumptions are necessary for the derivation of modelling input values. The impact of the assumptions on numerical outputs is minimised through a calibration and verification process against field observations. That is, the benchmark LTCC model sufficiently captures the top coal stability from initial extraction (i.e., face distance of top coal first caving) to cyclic extraction (i.e., failure extent ahead of coal wall). As a result, the top coal stability under possible variations of discrete fractures and coal seam characteristics can be quantified with confidence through newly developed stability indices (top coal fall rate and top coal recovery rate). It should be noted that during model development, very small blocks can be formed when fracture geometry varies, and they may cause unrealistic top coal fall/top coal recovery index. Although the current fall/recovery index excludes very small blocks, an advanced index representing not only quantity but also the quality of the fall/caving is recommended for more comprehensive analysis in separate studies. Face spall, which can contribute to top coal fall, should also be considered in future studies.

This paper presents a better understanding of longwall top coal stability both ahead of shield support (top coal fall) and behind shield support (top coal caving) when discrete fractures and coal seam characteristics vary in practice. The study demonstrates that the existence of discrete fractures decreases the top coal stability ahead of shield support, particularly in initial face extraction. The parametric study finds that when the fracture orientation makes an angle of 90 degrees to the positive x-axis, it has the least impact on top coal fall. When the fractures plunge into the mined-out area, they facilitate top coal caving and vice versa when they plunge into the unmined area. The study reveals that the fracture density is directly proportional to top coal fall and top coal caving. Meanwhile, the fracture stiffness and strength are inversely proportional to both top coal fall and caving. The study also demonstrates the important role of coal seam characteristics (strength, elastic modulus, and depth) in top coal fall. The findings from this paper can assist engineers in improving panel geometry design and roof control for efficient underground mining when discrete fractures exist and vary in the coal seam.

References

Cao, W. (2019). *Monitoring and Modelling of Microseismicity Associated with Rock Burst and Gas Outburst Hazards in Coal Mines*. (PhD Thesis), Royal School of Mines, London.

Dao, H. Q. (2010). *The effect of seam dip on the application of the Longwall Top Coal Caving method for inclined thick seams.* (PhD Thesis), The University of New South Wales, Sydney.

Frith, R. (2005). *Half a career trying to understand why the roof along the longwall face falls in from time to time?* Paper presented at the 24th International Conference on Ground Control in Mining, Morgantown.

Galvin, J. M. (2016). *Ground engineering - Principles and practices for underground coal mining*. Cham: Springer International Publishing.

Grey, I., & Gibbons, T. (2020). *Longwall behaviour in massive strata*. Paper presented at the The 2020 Coal Operators' Conference, University of Wollongong, Wollongong.

Ha Lam Coal Company. (2015). *Geotechnical design of Panel 11-1.14*. Quang Ninh: Ha Lam Coal Company.

Hebblewhite, B., Simonis, A., & Cai, Y. (2002). *Technology and feasibility of potential underground thick seam mining methods* (ACARP Project C8009). NSW, Australia.

Hoyer, D. I. (2011). *Early warning of longwall weighting events and roof cavities using LVA software*. Paper presented at the International Conference on Ground Control in Mining, Morgantown.

Iannacchione, A., Prosser, L., Esterhuizen, G., & Bajpayee, T. (2007). Methods for determining roof fall risk in underground mines. *Mining Engineering*, 59(11), 47-53.

Itasca Consulting Group. (2019). *UDEC – Universal Distinct Element Code, Ver. 7.0*. Minneapolis: Itasca.

Jasiulek, D., Bartoszek, S., Perůtka, K., Korshunov, A., Jagoda, J., & Płonka, M. (2019). Shield Support Monitoring System – operation during the support setting. *Acta Montanistica Slovaca*, 24(4), 391-401.

Langosch, U., Ruppel, U., & Witthaus, H. (2003). *Longwall roof fall prediction and shield support recommendations*. Paper presented at the 22nd International Conference on Ground Control in Mining, Morgantown.

Le, T. D., Bui, M. T., Pham, D. H., Vu, T. T., & Dao, V. C. (2018). A modelling technique for top coal fall ahead of face support in mechanised longwall using Discrete Element Method. *Journal of Mining and Earth Sciences*, 59(6), 56-65.

Le, T. D., Mitra, R., Oh, J., & Hebblewhite, B. (2017). A review of cavability evaluation in longwall top coal caving. *International Journal of Mining Science and Technology*, 27(6), 907-915. https://doi.org/10.1016/j.ijmst.2017.06.021.

Le, T. D., Vu, D. H., & Nguyen, A. T. (2020). Characteristics of top coal fall in front of face support in longwall: A case study. *Vietnam Journal of Earth Sciences*, 42(2), 152-161. https://doi.org/10.15625/0866-7187/42/2/14955.

McNally, G. H. (1996). *Estimation of the geomechanical properties of coal measures rocks for numerical modelling*. Paper presented at the Symposium on Geology in Longwall Mining, Sydney.

Medhurst, T., Hatherly, P., & Hoyer, D. (2014). *Investigation of the relationship between strata characteristics and longwall caving behavior*. Paper presented at the 14th Coal Operators' Conference, Wollongong.

Mohammad, N., Reddish, D. J., & Stace, L. R. (1997). The relation between in situ and laboratory rock properties used in numerical modelling. *International Journal of Rock Mechanics and Mining Sciences*, 34(2), 289-297. http://dx.doi.org/10.1016/S0148-9062(96)00060-5.

Palei, S. K., & Das, S. K. (2008). Sensitivity analysis of support safety factor for predicting the effects of contributing parameters on roof falls in underground coal mines. *International Journal of Coal Geology*, 75(4), 241-247. https://doi.org/10.1016/j.coal.2008.05.004.

Pappas, D., & Mark, C. (2011). Roof and rib fall incident trends: a 10-year profile. *Trans. Soc. Min. Metall. and Explor.*, 330, 462-478.

Paul, B. (2010). *Prospects for coal and clean coal technologies in Vietnam*, IEA Clean Coal Centre.

Payne, D. (2008). *Crinum Mine, 15 longwalls 40 million tonnes 45 roof falls - what did we learn?* Paper presented at the Coal 2008: Coal Operators' Conference, Wollongong.

Peng, S. S. (2008). *Coal mine ground control* (3rd ed.). Morgantown: West Virginia University.

Pham, D. H. (2012). *Development of geomechanical database for mechanisation of coal industry in Vietnam* (ĐT.02.10/ĐMCNKK). Hanoi: Institute of Mining Science and Technology.

Prusek, S., Rajwa, S., Wrana, A., & Krzemień, A. (2017). Assessment of roof fall risk in longwall coal mines. *International Journal of Mining, Reclamation and Environment*, 31(8), 558-574. https://doi.org/10.1080/17480930.2016.1200897.

Rafiee, R., Ataei, M., KhalooKakaie, R., Jalali, S. E., Sereshki, F., & Noroozi, M. (2018). Numerical modeling of influence parameters in cavabililty of rock mass in block caving mines. *International Journal of Rock Mechanics and Mining Sciences*, 105, 22-27. https://doi.org/10.1016/j.ijrmms.2018.03.001.

Rajwa, S., Janoszek, T., & Prusek, S. (2020). Model tests of the effect of active roof support on the working stability of a longwall. *Computers and Geotechnics*, 118, 103302. https://doi.org/10.1016/j.compgeo.2019.103302.

Trueman, R., & Hutchinson, I. (2018). The use of shield monitoring data for predicting in advance roof control problems on longwall faces. *Mining Technology*, 127(4), 209-218. https://10.1080/25726668.2018.1458478.

Vakili, A., Sandy, M., & Albrecht, J. (2012). *Interpretation of non-linear numerical models in geomechanics - a case study in the application of numerical modelling for raise bored shaft design in a highly stressed and foliated rock mass*. Paper presented at the 6th International Conference on Mass Mining, Sudbury.

Vervoort, A. (1988). Influence of longwall support on the occurrence of roof cavities. *International Journal of Mining and Geological Engineering*, 6(4), 313-326. https://doi.org/10.1007/BF00880929.

Wang, J., Wang, Z., & Li, Y. (2020). Longwall Top Coal Caving Mechanisms in the Fractured Thick Coal Seam. *International Journal of Geomechanics*, 20(8), 06020017. https://doi.org/10.1061/(ASCE)GM.1943-5622.0001722.

Xu, Q., Zhao, Y., & Li, Y. (2015). Statistical analysis and precautions of coal mine accidents in China. *Coal Engineering*, 47(3), 80-82 (in Chinese).

Yang, J. X., Liu, C. Y., & Yu, B. (2017a). The interaction between face support and surrounding rock and its rib weakening mechanism in hard coal seam. *Acta Montanistica Slovaca*, 22(1), 67-78.

Yang, X.-X., Jing, H.-W., Tang, C.-A., & Yang, S.-Q. (2017b). Effect of parallel joint interaction on mechanical behavior of jointed rock mass models. *International Journal of Rock Mechanics and Mining Sciences*, 92, 40-53. https://doi.org/10.1016/j.ijrmms.2016.12.010.